



Generating A Multiple Focal Hole using A Phase Modulated Azimuthally Polarized Laguerre Bessel Gaussian Beam

J. William Charles¹, M. Udhayakumar², K. B. Rajesh^{3*}, M. Lavanya⁴, A. Mohamed Musthafa⁵

^{1,2,*3}Department of Physics, Chikkanna Government Arts College, Trippur, TN, India.

⁴Department of Physics, PSGR Krishnammal College for Women, Coimbatore, TN, India.

⁵Department of General Studies (Physics Group), Jubail University College (Male Branch), Royal Commission of Jubail, Kingdom of Saudi Arabia.

Received: 21.08.2019

Accepted: 25.09.2018

Abstract

We propose a new approach for generating a multiple focal hole segment of subwavelength size, by tight focusing of a phase modulated azimuthally polarized Laguerre Bessel Gaussian beam (APLBGB). The focusing properties are investigated theoretically by vector diffraction theory. We observe that the focal hole segment with multiple focal structures separated with different axial distances can be generate by properly tuning the phase of the incident azimuthally polarized Laguerre Bessel Gaussian beam. We presume that such multiple focal whole patterns may find applications in atom optics, optical manipulations and multiple optical trapping.

Keywords: Fluorescence microscopy.

1. INTRODUCTION

The three-dimensional gradient force optical tweezers demonstrated by Ashkin *et al.* in 1986 has proven to be very useful tool for the manipulation of microscopic objects having refractive index higher than that of the surrounding medium (high index particle) (Sasaki *et al.* 1992). Such a tweezers, however, cannot be used for trapping microscopic particles of refractive index lower than that of the surrounding medium (low index particles), because these get repelled away from the regions of the highest intensity. The ability to trap and manipulate such low-index Particles would allow for the trapping of bubbles and droplets so that their evolution in different liquid media could be investigated. Since low index particles such as bubbles are of considerable interest for their potential application in the field of biology and medicine. For example, recently enhancement of cell permeability caused by localized cell damage induced by the asymmetric collapse of a bubble has been used for drug delivery and transfection of genes into the living cells (Gahagan and Swartzlander, 1996). Since the cavitation damage by a collapsing bubble depends on its relative to trap and manipulate low index particles (Ashkin and Dziedzic, 1989) may enhance the understanding of bubble

dynamics and optimize the extent of cell damage caused by bubbles. Similarly low index particles are also finding use as contrast agents (Wright *et al.* 1990), and for selective destruction of cancer cells (Tadir *et al.* 1990) separation from the surface. Moreover, the conventional gradient-force trap based on the design of Ashkin *et al.* has some limitations such as the trapped particles are susceptible to optical damage by absorptive heating because the center of the trap is located in the high-intensity focal region of the beam. This hinder the earlier suggestion of biomedical and related applications involving micromanipulation of living cells, (Block *et al.* 1990) chromosomes, (Swoboda *et al.* 1993) spermatozoa, (Tadgubana *et al.* 1999) and motor proteins. (Ye *et al.* 2004; Prentice *et al.* 2005). One basic approach for trapping low index particles is to generate a region of lower intensity, surrounded by a higher intensity region. Optical bottle fields also have applications in stimulated emission depletion (STED) fluorescence microscopy (De Jong *et al.* 2002), in which the three-dimensional nature of the bottle provides enhanced resolution along the longitudinal direction (Hell and Wichmann, 1994; Lenz *et al.* 1994). Various techniques have been proposed to generate bottle fields (Suyama and Zhang, 2013; Shvedov *et al.* 2008; Chen *et al.* 2004; Zhang *et al.* 2011). Many of

* K. B. Rajesh

email: rajeshkb@gmail.com

these involve vortices generated by the use of phase masks, spiral phase plates, or spatial light modulators (Loiko *et al.* 2013; Gbur and Visser, 2003). These methods typically rely on interference between two fundamental Gaussian modes, making them sensitive to alignment errors (Mahou *et al.* 2015). In 2000, Tovar proposed new Laguerre–Bessel–Gaussian (LBG) beams as solutions of the paraxial wave equation in cylindrical coordinates (Tovar, 2000). The LBG beams can reduce to the BG modes and LG modes by properly tuning the initial parameters. Subsequently, the non-paraxial propagation properties of vectorial LBG beams were researched based on vectorial Rayleigh–Sommerfeld formulas (Mei and Zhao, 2007). Recently, the tight focusing properties of radially polarized Laguerre–Bessel–Gaussian beams by a high numerical aperture objective in the immersion liquid is analyzed based on the vector diffraction theory. In this work, based on the vector diffraction theory, we suggested a novel method to

trap low refractive index particles using a azimuthally polarized Laguerre Bessel Gaussian Beam phase modulated with well optimized phase filters. It is observed that by suitably modifying the phase of the incident beam using a multi belt complex phase filter (MBCPF), one can generate multiple focal hole patterns with different sub-wavelength dimensions and large focal depth that finds applications in multiple optical trapping and atom optics application.

2. THEORY

The analysis was performed by numerically evaluating Richards and Wolf's vectorial diffraction equation widely used for high NA focusing systems (Richards and Wolf, 1959). The electric field distribution in the vicinity of focus for the incident azimuthally polarized beam is given by

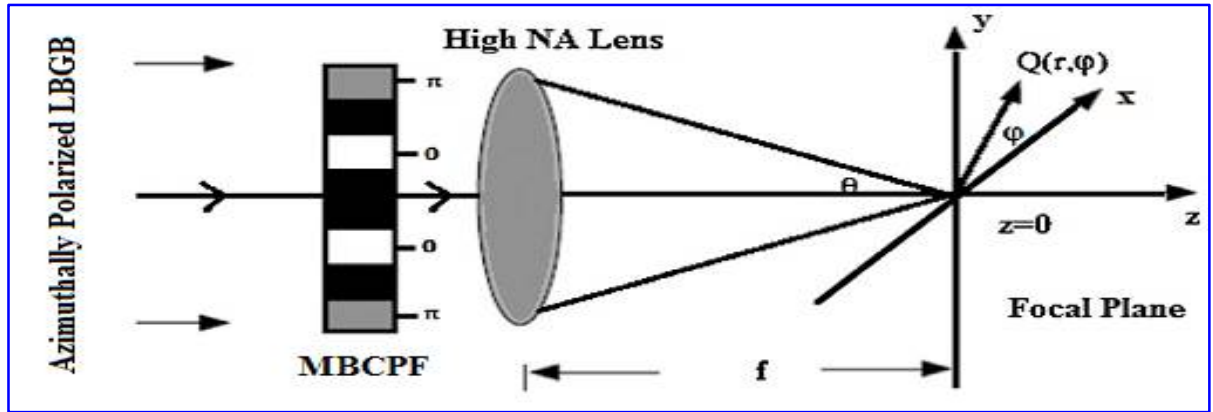


Fig. 1: Tight focusing properties of azimuthally polarized Laguerre Bessel Gaussian beam passes through a complex phase filter and is subsequently focused by a high-NA lens

$$E(r, \varphi, z) = \begin{bmatrix} E_r \\ E_\varphi \\ E_z \end{bmatrix} = \left[2A \int_0^\alpha \cos^{1/2}(\theta) \sin(\theta) A(\theta) J_1(kr \sin \theta) e^{ikz \cos \theta} d\theta \right] \rightarrow (1)$$

where A is relative amplitude, $\theta_{\max} = \arcsin(NA/n)$ that is the maximum aperture angle with (NA/n) is the ratio of numerical aperture (NA) and n is the index of refraction between the lens and the sample. k is the wave number in free space. $J_n(\theta)$ denotes the n th-order Bessel function and the function of $T(\theta)$ describe the amplitude modulation. In the focusing system with a

high NA objective lens we investigated, the focusing beam of light is an azimuthally polarized LBG beam. In the cylindrical coordinate system (r, φ, z) , the pupil function $l(\theta)$ for a azimuthally polarized LBG beam at the source plane $z=0$ can be defined as (Mei and Zhao, 2007).

$$l(\theta) = \frac{\beta^2 \sin \theta}{\sin \theta_{\max}} L_0^1 \left(\frac{2\beta^2 \sin^2 \theta}{\sin \theta_{\max}} \right) J_1 \left(2\beta \frac{\sin \theta}{\sin \theta_{\max}} \right) \times \exp \left(-\frac{\beta^2 \sin^2 \theta}{\sin \theta_{\max}} \right) \rightarrow (2)$$

With β , which is the truncation parameter which is defined as the ratio of pupil to beam waist in front of the focusing objective. $\theta_{max} = \arcsin(NA/n)$ represents the maximum value of the convergence angle θ , n is the refraction in the image plane, L_0^1 Denotes the Laguerre polynomial with the radial and angular modes of 0 and 1, and J_1 is the Bessel function of the first kind of order one, respectively. The dedicated Multi Complex Phase Filter (MBCPF) is shown in fig 6.1. The MBCPF is the combination of phase and amplitude filter which has 4 belts in the radial direction. They are reported as the most useful DOEs to decrease the focal spot size and to improve the focal depth (Prabakaran *et al.* 2014). The effect multi belt complex phase filter on the input azimuthally polarized LBGB is evaluated by $T(\theta)$

$$T(\theta) = \begin{cases} 0, & \text{for } 0 < \theta < \theta_1, \theta_2 < \theta < \theta_3, \\ 1, & \text{for } \theta_1 < \theta < \theta_2, \\ -1 & \text{for } \theta_3 < \theta < \theta_{max} \end{cases} \rightarrow (3)$$

Here we considered the 4 belt spiral phase hologram and the set of four angles are optimized to obtain a particular focal patterns using traditional global-search-optimization algorithm (Wang *et al.* 2008). Based on this algorithm, we normally choose one structure with random values for θ_1 to θ_3 from all possibilities; we then numerically simulate their focusing properties using vector diffraction theory. If the structure generates a sub wavelength single focal spot as expected and

satisfies the limiting conditions that that the Full Width Half Maximum (FWHM) of the generated focal spot segment is less than 0.5λ , it is fixed as the initial structure during the optimization procedures. In the following steps, we then continue to vary θ of one chosen zone slowly and in precise increment to generate multiple focal spots segments without violating the limiting conditions that that the FWHM of each of the generated focal spot is less than 0.5λ and there should be at least five, three or two such focal spots in the focal segment.

3. RESULTS & DISCUSSION

A schematic diagram of the proposed method is shown in Fig. 1. We perform the numerical evaluation of Eq. (6.1) by setting the parameters $\lambda = 1$ and NA of the objective as 0.95. Here, for simplicity, we assume that the focusing is on air and the refractive index n is 1 and the refractive amplitude A is 1. In the following step, we continue to increment θ of chosen zone to generate double focal hole segment without changing the limiting condition. Fig. 2 illustrate the formation of two focal hole segment generated by the high NA lens for the CPF optimized with angle $\theta_1 = 50.90^\circ$, $\theta_2 = 56.85^\circ$ and $\theta_3 = 60.83^\circ$ for $\beta = 1.1$. It is observed from Fig. 2(c) that the each of the generated focal hole poses focal depth around 4.4λ and the FWHM of each ring is 0.37λ . The axial distance between two focal hole structures is measured as 2.1λ and are measured at $r = 0.35\lambda$ as shown in Fig. 2(b).

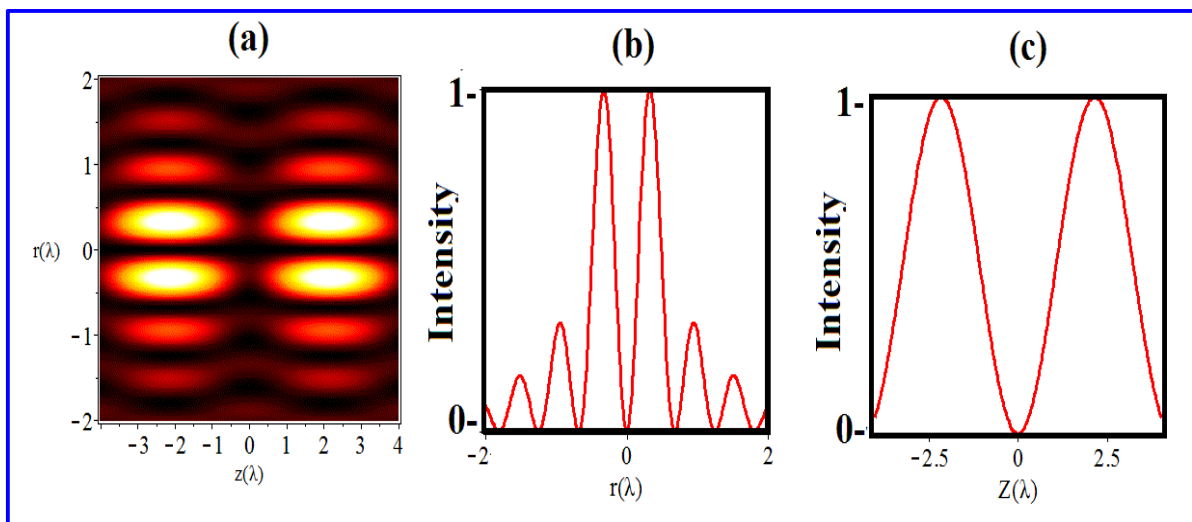


Fig. 2: (a) The 2D normalized intensity distribution in the r - z plane (b) The total intensity distribution at $z = 2.1\lambda$ (c) The axial intensity distribution at $r = 0.35\lambda$.

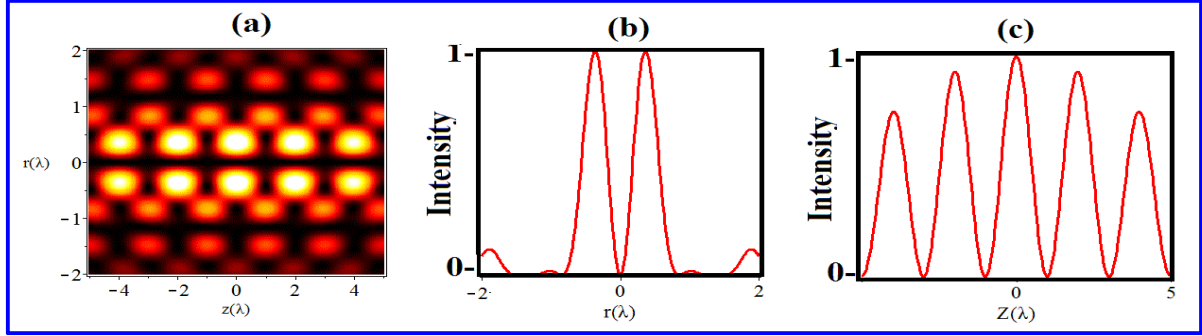


Fig. 3: (a) The normalized intensity distribution in the r - z plane (b) The total intensity distribution at $z = 2\lambda$ (c) The axial intensity distribution at $r = 0.35\lambda$.

Fig. (3) shows the multiple focal hole segment generated by the high NA lens for the CPM with for $\beta = 1.1$. It is observed from the figure that the generated focal segment contains array of five focal hole each having FWHM of 0.37λ with d of around 1.2λ and axially are separated by the distance $z=2\lambda$. These angles are optimized based on the procedure mentioned for the fig. 6.2, but with the limiting condition that the FWHM of the generated focal hole segment is less than 0.5, and there should be at least five such focal holes in the focal segment.

Fig. 4. shows the possibility of obtaining series of sub wavelength scale focal hole segment of slightly different FWHM aligned alternatively along the axial direction. We noted that such a focal segment can be generated with the CPF optimized with angle $\theta_1 = 39.06^\circ$, $\theta_2 = 42.12^\circ$ and $\theta_3 = 60.83^\circ$. Fig. (3b) shows the FWHM of inner focal holes is 0.38λ where the larger located alternatively to this is FWHM of 0.8λ . The on axial intensity measured at $r=0.35\lambda$ shows that the intensity of the focal hole at the focus is maximum and fades exponentially along the longitudinal axis.

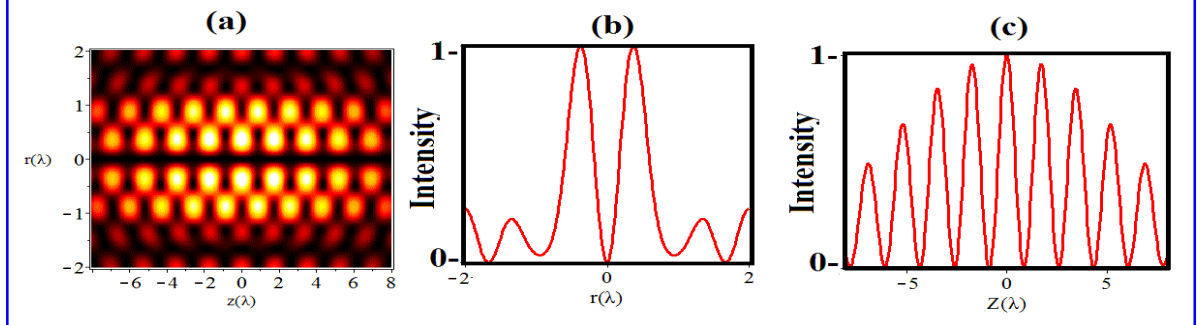


Fig. 4: (a) The normalized intensity distribution for multiple focal hole segment. (b) The total intensity distribution at $z = 0$. (c) The axial intensity distribution at $r = 0.35$

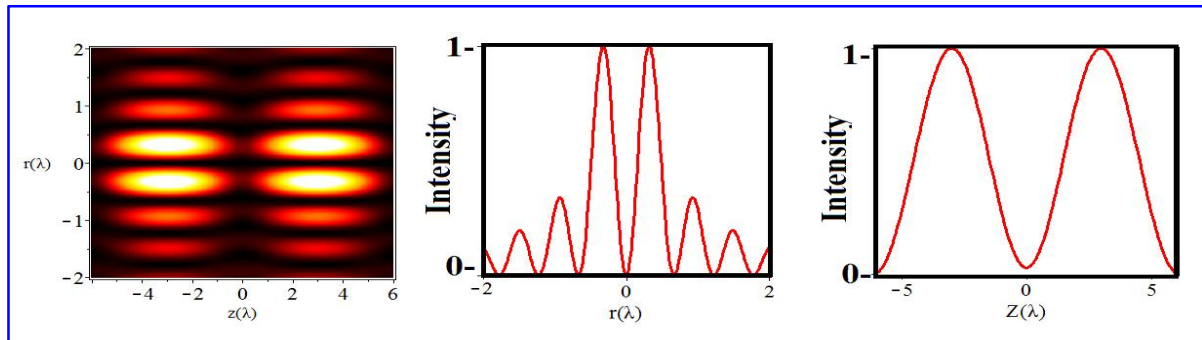


Fig. 5: (a) The normalized intensity distribution in the r - z plane (b) The total intensity distribution at $z = 3\lambda$ (c) The axial intensity distribution at $r = 0.35\lambda$

Fig. 5(a) shows that the focal segment obtained for the CPF optimized with angle $\theta_1 = 36.06^\circ$, $\theta_2 = 41.12^\circ$ and $\theta_3 = 48.83^\circ$. It is observed from figure the generated focal hole is having FWHM of 0.33λ and focal depth of 2.8λ . It is noted the on axial intensity of the focal hole is equal and are axially separated by the distance 2.5λ . Hence we can generated array of

almost equally intense and uniformly spaced sub wavelength focal hole segment which can be used trap two low refractive index particles simultaneously. Thus by modulating the pupil beam ratio of incident LBG for well optimized complex phase filter one can also generate many novel focal patterns that suitable for trapping of multiple low refractive index particle.

Table 1. showing the details of the focal patterns obtained for phase modulated APLBG beam

S.No	APLBG (β)	Optimized angle of CPF	Number of Focal holes	FWHM (λ)	DOF (λ)	Axial separation (λ)
1	1.1	$\theta_1 = 50.90^\circ$, $\theta_2 = 56.85^\circ$ and $\theta_3 = 60.83^\circ$	2	0.37	4.4	2.5
2	1.1	$\theta_1 = 39.06^\circ$, $\theta_2 = 42.12^\circ$ and $\theta_3 = 48.83^\circ$	5	0.37	1.2	2
3	1.1	$\theta_1 = 39.06^\circ$, $\theta_2 = 42.12^\circ$ and $\theta_3 = 60.83^\circ$	9	0.34	0.8	2
4	1.1	$\theta_1 = 56.06^\circ$, $\theta_2 = 58.12^\circ$ and $\theta_3 = 60.83^\circ$	2	0.35	2.8	3.1

4. CONCLUSION

In conclusion the tight focusing properties of azimuthally polarized LBGGB focused through a well optimized complex phase filter is illustrated numerically using vector diffraction theory. Numerical result shows that by suitably modulating the phase of the CPF and suitably modulating pupil beam ratio of the incident APLBGGB, there is a possibility to achieve many novel focal pattern such as splitting of focal hole segment into array of two or five focal hole segment. We also noted that the focal segment with slightly different FWHM arranged uniformly and alternatively can also be achieved.

REFERENCES

- Ashkin, A. and Dziedzic, J. M., Optical trapping and manipulation of single living cells using infra-red laser beams, *Ber. Bunsenges. Phys. Chem.*, 93(3), 254 (1989).
[doi:10.1002/bbpc.19890930308](https://doi.org/10.1002/bbpc.19890930308)
- Block, S. M., Goldstein, L. S. and Schnapp, B. J., Bead movement by single kinesin molecules studied with optical tweezers, *Nature (London)*, 348-352(1990).
[doi:10.1038/348348a0](https://doi.org/10.1038/348348a0)
- Chen, C.-H., Tai, P.-T. and Hsieh, W.-F., Bottle beam from a bare laser for single-beam trapping, *Appl. Opt.*, 43(32), 6001–6006(2004).
- De Jong, N., Bouakaz, A. and Frinking, A., Echocardiography, 19(3), 229 (2002).
[doi:10.1046/j.1540-8175.2002.00229.x](https://doi.org/10.1046/j.1540-8175.2002.00229.x)
- Gahagan, K. T. and Swartzlander, G. A., Optical vortex trapping of particles, *Opt. Lett.*, 21(11), 827-829(1996).
[doi:10.1364/OL.21.000827](https://doi.org/10.1364/OL.21.000827)
- Gbur, G. and Visser, T. D., Coherence vortices in partially coherent beams, *Opt. Comm.*, 222(1-6), 117–125(2003).
[doi:10.1016/S0030-4018\(03\)01606-7](https://doi.org/10.1016/S0030-4018(03)01606-7)
- Hell, S. W. and Wichmann, J., Breaking the diffraction resolution limit by stimulated emission: stimulated-emission depletion fluorescence microscopy, *Opt. Lett.*, 19(11), 780–782(1994).
[doi:10.1364/OL.19.000780](https://doi.org/10.1364/OL.19.000780)
- Lenz, M. O., Sinclair, H. G., Savell, A., Clegg, J. H., Brown, A. C., Davis, D. M., Dunsby, C., Neil, M. A. and French, P. M., 3-D stimulated emission depletion microscopy with programmable aberration correction, *J. Biophotonics*, 7(1-2), 29–36 (2014).
[doi: 10.1002/jbio.201300041](https://doi.org/10.1002/jbio.201300041)
- Loiko, Y. V., Turpin, A., Kalkandjiev, T., Rafailov, E.U. and Mompart, J., Generating a three-dimensional dark focus from a single conically refracted light beam, *Opt. Lett.*, 38(22), 4648–4651 (2013).
[doi:10.1364/OL.38.004648](https://doi.org/10.1364/OL.38.004648)
- Mei, Z. and Zhao, D., Nonparaxial analysis of vectorial Laguerre–Bessel–Gaussian beams, *Opt. Express*, 15(19), 11942–11951(2007).
[doi:10.1364/OE.15.011942](https://doi.org/10.1364/OE.15.011942)

- Prabakaran, K., Rajesh, K. B. and Pillai, T. V. S., Generation of multiple sub wavelength focal spot segments using radially polarized Bessel Gaussian beam with complex phase filter, *Optik-International Journal for Light and Electron Optics*, 125(13), 3159-3161(2014).
[doi:10.1016/j.ijleo.2013.12.009](https://doi.org/10.1016/j.ijleo.2013.12.009)
- Prentice, P., Cuschieri, A., Dholakia, K., Prausnitz, M. and Campbell, P., Membrane disruption by optically controlled microbubble cavitation, *Nature Phys* 1, 107-110(2005).
doi.org/10.1038/nphys148
- Richards, B. and Wolf, E., Electromagnetic diffraction in optical systems. II. Structure of the image field in an aplanatic system, *Proc. R. Soc. Lond. Ser. A, Math. Phys. Sci.*, 253, 358-379(1959).
[doi:10.1098/rspa.1959.0200](https://doi.org/10.1098/rspa.1959.0200)
- Sasaki, K., Koshioka, M., Misawa, H., Kitamura, N. and Masuhara, H., Optical trapping of a metal particle and a water droplet by a scanning laser beam, *Appl. Phys. Lett.*, 60, 807(1992).
[doi:10.1063/1.107427](https://doi.org/10.1063/1.107427)
- Shvedov, V. G., Izdebskaya, Y. V., Rode, A. V., Desyatnikov, A., Krolikowski, W. and Kivshar, Y. S., Generation of optical bottle beams by incoherent white-light vortices, *Opt. Express*, 16(25), 20902-20907(2008).
[doi:10.1364/OE.16.020902](https://doi.org/10.1364/OE.16.020902)
- Suyama, T. and Zhang, Y., 3D super-resolution fluorescence microscopy using cylindrical vector beams, *Prog. Electromagn. Res. Lett.*, 43, 73-81(2013).
[doi:10.2528/PIERL13080205](https://doi.org/10.2528/PIERL13080205)
- Svoboda, K., Schmidt, C. F. and Schnapp, B. J. and Steven, M., Direct observation of kinesin stepping by optical trapping interferometry, *Nature (London)*, 365,721-727(1993).
[doi:10.1038/365721a0](https://doi.org/10.1038/365721a0)
- Tachibana, K., Uchida, T., Ogawa, K., Yamashita, N. and Tamura, K., Induction of cell-membrance porosity by ultrasound, *Lancet*, 353(9162), 1409-1415(1999).
[doi:10.1016/S0140-6736\(99\)01244-1](https://doi.org/10.1016/S0140-6736(99)01244-1)
- Tadir, Y., Wright, W. H., Vafa, O., Ord, T., Asch, R. H. and Berns, M. W., Micromanipulation of sperm by a kaser generated optical trap, *Fertil Steril.*, 52(5), 870-873(1989).
- Tovar, A. A., Propagation of Laguerre-Bessel-Gaussian beams, *J. Opt. Soc. Am. A.*, 17(11), 2010-2018(2000).
[doi:10.1364/JOSAA.17.002010](https://doi.org/10.1364/JOSAA.17.002010)
- Wang, H., Shi, L., Lukyanchuk, B., Sheppard, C. and Chong, C. T., Creation of a needle of longitudinally polarized light in vacuum using binary optics, *Nat. Photonics*, 2, 501-505 (2008).
[doi:10.1038/nphoton.2008.127](https://doi.org/10.1038/nphoton.2008.127)
- Wright, W. H., Sonek, G. J., Tadir, Y. and Berns, M. W., *IEEE J. Quantum Electron.*, 26(12), 2148-2157(1990).
[doi:10.1109/3.64351](https://doi.org/10.1109/3.64351)
- Ye, J. Y., Chang, G., Norris, T. B., Tse, C., Zohdy, M. J., Hollman, K. W., O'Donnell, M. and Baker, J. R., Trapping cavitation bubbles with a self-focused laser beam, *Opt. Lett.*, 2(18), 2316-2138(2004).
[doi:10.1364/ol.29.002136](https://doi.org/10.1364/ol.29.002136)
- Youngworth, K. S. and Brown, T. G., Focusing of high numerical aperture cylindricalvector beams, *Opt. Express*, 7(2), 77-87(2000).
[doi:10.1364/OE.7.000077](https://doi.org/10.1364/OE.7.000077)
- Zhang, P., Zhang, Z., Prakash, J., Huang, S., Hernandez, D., Salazar, M., Christodoulides, D. N. and Chen, Z., Trapping and transporting aerosols with a single optical bottle beam generated by moiré techniques, *Opt. Lett.*, 36(8), 1491-1493(2011).
[doi:10.1364/OL.36.001491](https://doi.org/10.1364/OL.36.001491)